Automated Liver Elasticity Calculation for 3D MRE

Bogdan Dzyubak, **Kevin J. Glaser**, **Armando Manduca**, and **Richard L. Ehman**

Department of Radiology, Mayo Clinic, Rochester, MN

Abstract

Magnetic Resonance Elastography (MRE) is a phase-contrast MRI technique which calculates quantitative stiffness images, called elastograms, by imaging the propagation of acoustic waves in tissues. It is used clinically to diagnose liver fibrosis. Automated analysis of MRE is difficult as the corresponding MRI magnitude images (which contain anatomical information) are affected by intensity inhomogeneity, motion artifact, and poor tissue- and edge-contrast. Additionally, areas with low wave amplitude must be excluded. An automated algorithm has already been successfully developed and validated for clinical 2D MRE. 3D MRE acquires substantially more data and, due to accelerated acquisition, has exacerbated image artifacts. Also, the current 3D MRE processing does not yield a confidence map to indicate MRE wave quality and guide ROI selection, as is the case in 2D. In this study, extension of the 2D automated method, with a simple wave-amplitude metric, was developed and validated against an expert reader in a set of 57 patient exams with both 2D and 3D MRE. The stiffness discrepancy with the expert for 3D MRE was $-0.8\% \pm 9.45\%$ and was better than discrepancy with the same reader for 2D MRE ($-3.2\% \pm 10.43\%$), and better than the inter-reader discrepancy observed in previous studies. There were no automated processing failures in this dataset. Thus, the automated liver elasticity calculation (ALEC) algorithm is able to calculate stiffness from 3D MRE data with minimal bias and good precision, while enabling stiffness measurements to be fully reproducible and to be easily performed on the large 3D MRE datasets.

Keywords

MRE; Elastography; Segmentation; Automation; ROI; Liver; CAD; Stiffness

1. INTRODUCTION

Hepatic fibrosis is a significant world health problem causing as many as 44,000 deaths and over 100,000 acute hospitalizations annually in the US alone [1]. Magnetic Resonance Elastography (MRE) [2] has been shown to have a high sensitivity and specificity for diagnosing hepatic fibrosis [3] and is gradually replacing liver biopsy, which is invasive and prone to sampling error, as the diagnostic method of choice. During an MRE exam, a steady-state acoustic wave (typically at 60 Hz) is introduced into the body using a driver (a pneumatic speaker strapped to the patient's chest) and imaged using phase-contrast MRI. The acquisition generates axial magnitude images, which contain anatomical information, and phase images, which capture displacement information about the through-plane tissue motion to visualize shear waves propagating in the imaging plane. An MRE inversion then calculates a quantitative elastogram. A typical MRE dataset is shown in Figure 1.

The inversion can be biased in areas where the magnitude image SNR and/or wave amplitude is low, as well as in areas with partial volume or other artifact. Therefore, the liver stiffness is calculated from a carefully selected ROI. Commonly, ROIs are drawn by experienced readers but the procedure is subjective and results in an inter-reader stiffness variability of 10% [4], which is the largest factor in the variability of the MRE exam. In an earlier study, we presented and validated an Automated Liver Elasticity Calculation (ALEC) algorithm to remove reader variability. It had a higher agreement with an expert than did experienced clinical technicians [5], and is presently used for all clinical liver stiffness calculation at our institution.

A new MRE acquisition and inversion, 3D MRE, has recently been developed to further improve the accuracy and reproducibility of liver MRE. This method acquires higher-resolution isotropic voxels and encodes wave propagation in all three directions rather than just within the imaging slice. This provides more accurate elastograms by removing the biased stiffness results from imaging waves propagating obliquely through the imaging plane, and also allows more sophisticated processing to be performed. In the liver, the primary benefit of 3D MRE is enabling tumors (which can occur as a result of liver disease) to be characterized more accurately in the same acquisition that was used to stage liver disease. 3D MRE produces substantially more images for analysis, having 32 isotropic slices instead of 4 and 3 directions of motion encoding instead of 1. This large multi-directional dataset is cumbersome for a human reader to analyze. Thus, extension of the automated processing to 3D MRE would be useful to improve the convenience, accuracy, and reproducibility of analyzing 3D MRE data.

3D MRE data poses additional challenges compared to the standard 2D MRE data. An accelerated spin-echo echo-planar (EPI) pulse sequence, and a smaller acquisition matrix (96x96 vs 256x128), later interpolated to the same image size (256x256), are used to acquire 3D data in the same time as 2D (roughly 1 minute). As a result, the images have exacerbated blurring, intensity inhomogeneity, and low tissue-contrast. Furthermore, the confidence map, calculated by the 2D MRE inversion to guide manual ROI selection, is not available in 3D due to computational costs. This study tests the applicability of the automated method, with the confidence map alternative, to 3D MRE data by comparing the liver stiffnesses that it calculates to an expert human reader.

2. METHODS

2.1 MRE Data

An MRE dataset consists of magnitude images, similar to standard anatomical MRI images but with lower image quality, and phase images, which contain information about the propagation of cyclic mechanical waves introduced into the body. The acquisitions for 2D MRE and 3D MRE are described in [4, 6]. The main relevant differences are that the 3D images tend to have lower resolution, poorer tissue-contrast and intensity homogeneity, and the processing algorithm does not provide a wave-quality metric to help guide ROI placement. Several magnitude/phase image pairs (typically 4 in 2D MRE and 3 in 3D MRE) are acquired for each imaging slice with different offsets between the start of the motion and the start of the motion encoding gradients to capture snapshots of the wave propagation at

different points in the cycle. The stiffness inversion processing uses these multiple phase-offsets to calculate elastograms with quantitative stiffness values for every voxel.

If the wave SNR is low, the elastogram can be biased, either regionally or globally. Low SNR can result from low-amplitude motion, caused by an inactive/decoupled acoustic driver or highly attenuating liver, or from low magnitude image signal, caused, for example, by high iron content in the patient's liver. A confidence map is calculated by the inversion in 2D MRE to indicate and exclude areas of low wave SNR. For a 3D MRE dataset, the confidence map is not generated in a typical workflow due to computation costs. As a result, the manual ROI selection technique in 3D MRE does not rely on a quantitative data quality metric for guidance and is more approximate, favoring regions near the external edge of the liver which are close to the acoustic driver and are likely to have higher wave amplitude. The automated technique in 2D uses the confidence map, but a new method, described below, needed to be developed for 3D data.

2.2 Algorithm

The automated MRE processing, described in detail in [5], consists of the following steps performed on the 2D slices of the dataset (Figure 2):

1. **Initialization:** Voxels with intensities within the lower 5th percentile were pre-labeled as background and eroded by 7 pixels. Basic segmentation of abdominal fat was performed by eroding layers from the outside of the body contour until a change in intensity was detected, indicating the transition between the abdominal fat and the abdominal organs/cavities. Liver was labeled as voxels internal to the abdominal fat segmentation, brighter than background, and on the top-left side of the body in the image (anterior-right side of the body). A set of three intensity membership functions was then constructed for these three classes by setting membership to 1 at the average intensity of the voxels labeled as that class and linearly decreasing membership until it reached zero at the mean intensities of nearby classes. For background, the membership was kept at one for intensities below its mean and for fat the membership was kept at 1 above the mean. Distances between the morphologically eroded background and fat masks, and fat and liver masks were used to construct spatial membership functions. The intensity and distance membership functions were multiplied together and used to reclassify all voxels into background, liver, fat, or other tissue. For 3D MRE, the only difference was to consider liver brighter than fat due to fat-suppression in the acquisition sequence. An example of the initialization membership functions are shown in Figure 2.

2. **Segmentation:** The resulting pre-segmentations were sub-sampled evenly to generate seeds for each class. A Random Walker segmentation [7] was then run on an intensity inhomogeneity-corrected [8] magnitude image to segment the liver (Figure 3).

3. **Confidence metric:** In 2D MRE, the standard confidence map calculated by the inversion and thresholded at 0.95 was used by the automated algorithm and also by the human reader during the ROI drawing. In 3D MRE, the expert did not use

a confidence metric. For the algorithm, the wave Amplitude-to-Noise (ANR) map was calculated as shown in the workflow of Figure 4:

The Fourier Transform of the evenly-spaced unwrapped phase-offset images across time was taken, and the second term was selected to choose motion at the applied principal frequency. This approach serves as a filter which removes bulk motion and some of the noise. The absolute value of this term is the vibrational amplitude. The amplitude image was smoothed using an 11x11 kernel to match the size of the 2D inversion processing kernel and the spatial extent of potential artifacts in the elastogram. Magnitude image SNR was then calculated by dividing a neighborhood average by the neighborhood standard deviation, both calculated using 11x11 kernels. The amplitude and the magnitude SNR were multiplied together to calculate the ANR map (Figure 5). The ANR map threshold below which voxels should be excluded from the final ROI was optimized by calculating the maps for all 2D MRE data sets and maximizing the Dice overlap coefficient of the thresholded ANR maps with the confidence maps thresholded at the standard value of 0.95. The average of optimal thresholds across all 2D MRE exams was calculated and used for thresholding the ANR in 3D data.

4. **Final ROI**: The liver segmentation and the thresholded confidence map (2D MRE), or ANR map (3D MRE), were used to calculate the final ROI within the liver as described in the original ALEC paper [5]. Briefly, the liver segmentation was eroded from edges and blood vessels, the confidence/ANR map was used for the masking of noisy or low-amplitude areas of the liver, and any regions with sharp changes in elasticity were removed, as the inversion assumes local homogeneity and is not expected to produce localized hard/soft regions in liver tissue except when there are poorly-visible tumors/vessels or severe wave interference.

2.3 Validation against the expert

A set of 57 patient exams which had both 2D MRE and 3D MRE images as well as ROIs manually calculated by an expert MRE reader with 5 years of experience were retrieved. The retrieved manual data contained ROIs for all 4 slices of 2D data and slices 7–26 (of the acquired 32 slices) of the 3D data, with the top and bottom slices excluded due to partial volume in the elastograms caused by the large inversion kernel. Average liver stiffnesses were calculated from these ROIs and used as reference for evaluating stiffnesses calculated using the automated method. For 3D data, automated processing was done only on slices 10, 14, 18, and 22 for faster computation.

Stiffness correlations and percent differences with the expert reader were calculated for 2D MRE (already validated) and 3D MRE (new). Failure rate, defined as the inability to obtain at least a 2000-voxel ROI across the 4 slices, when the expert reader has done so, or having a stiffness difference of >50% from the expert reader, was also recorded.

3. RESULTS

Of the 57 cases analyzed, ALEC did not fail in any 2D or 3D exam. The processing took, on average, 5 minutes for every 4-slice dataset. An example of the manual and the automated mask for a 3D MRE case is shown in Figure 6. The percent difference in stiffness from the expert reader for 3D MRE was $-0.8\% \pm 9.45\%$ ($\mu \pm \sigma$) which was slightly better than the difference in stiffness in 2D with the same reader ($-3.2\% \pm 10.43\%$). The intraclass correlation coefficient for automated vs manual stiffnesses was 0.983 for 3D MRE (Figure 7) and 0.972 for 2D MRE. The ANR took under a second to compute for a 4-slice exam, using phase images for the axial direction of wave-encoding. No substantial difference was observed between phase images of only one and of all three directions. The ANR map optimal threshold was 7, for phase data scaled $-2*\pi$ to $+2*\pi$, and yielded a Dice coefficient of 0.75 with thresholded standard confidence maps across the 2D dataset.

4. DISCUSSION AND CONCLUSIONS

The algorithm-to-expert agreement was very comparable between the 2D MRE and 3D MRE cases. Furthermore, it was slightly better than the agreement of clinical technicians with expert readers that was found in the original ALEC validation study [4]. Considering the high agreement and the fact that the automated processing did not fail in any cases we believe this approach to automated 3D MRE analysis to be successful.

It remains to be investigated whether the use of only a few slices affects the ability to calculate stiffness reproducibly. However, physiologically stiffness varies slowly, elastograms have low resolution due to the size of the processing kernel, and both automated and manual methods exclude areas with sharp changes in stiffness. Thus, although 3D MRE is useful for accurately performing the elasticity inversion without suffering from bias when waves propagate obliquely across slices, it may not be necessary to use all slices for the calculation of average liver stiffness. The calculation of stiffness from the full 20 central slices could be done within the clinical workflow, however, as a 30 minute delay in reporting stiffness after an acquisition is typically considered acceptable. Full 3D automated processing, as opposed to the slice-by-slice analysis performed currently, has the potential to increase the accuracy of the segmentation and artifact removal. However, the iterative inhomogeneity-correction and the Random Walker steps take a substantial amount of time for 3D volumes, so the benefit may not be worth the increased processing time. On the other hand, the initialization and the final ROI artifact exclusion can benefit from cross-slice awareness without adding substantially to the total processing time.

The ANR metric is relatively simple. It has the benefit of being very fast to calculate and thus it can easily incorporate the full information from multi-slice imaging and multiple directions of wave propagation. It also considers both of the main causes of potentially biased data - wave amplitude and noise level. Due to having a local standard deviation term in the denominator, the ANR will have low values near edges, making these areas more likely to be excluded. This property is useful and works independently and in parallel with the erosion of the segmented liver mask to exclude areas with partial volume-effects in the elastogram. More sophisticated metrics of wave quality can be derived, such as the

octahedral shear strain SNR [9]. The goal of this study was to evaluate the feasibility of a fully automated processing method on 3D MRE data, which was considered to be a success. The investigation of different wave-quality metrics and thresholds which will better allow biased values in the elastograms to be excluded sensitively and specifically is a topic of future work. The quality metric may also be useful as a standalone tool for guiding manual ROI drawing for cases when full automated processing is unavailable or unsuitable, for example, for calculating stiffness of tumors.

Earlier work aimed at automatically processing 3D MRE data has investigated various approaches such as registration-based segmentation [5]. However, ultimately the same methods used in the original ALEC algorithm were found to be effective and were used for 3D MRE processing to maintain consistency. The use of simple membership functions, instead of fit-based methods with many assumptions, allows ALEC to deal with intensity inhomogeneity, low inter-tissue contrast, blurring, and motion artifacts. A perfect liver segmentation is not attained in every case but this is not required – only a representative artifact-free ROI is needed for diagnosis. The intermediate liver segmentation step was not evaluated directly as the manual analysis directly produces the final ROI. Also, two experienced MRE readers can produce completely non-overlapping ROIs while obtaining the correct and diagnostically valuable liver stiffness. So, the comparison with the expert was done in terms of final liver stiffness values rather than ROI masks.

In summary, the algorithm described in this work was found to be a reliable and accurate method of calculating stiffness from 3D MRE images, having high expert-agreement and high success rate despite the very challenging image quality. The automated stiffness calculation removes the inter- and intra-reader discrepancy of manual interpretation and allows large 3D MRE datasets to be analyzed. Further improvements to the wave quality metric for 3D MRE are a subject of future work.

Acknowledgments

References

1. Bataller R, Brenner D. Liver fibrosis. J Clin Invest. 2005; 115(2):209–18. [PubMed: 15690074]

2. Muthupillai R, Lomas DJ, Rossman PJ, et al. Magnetic resonance elastography by direct visualization of propagating acoustic strain waves. Science. 1995; 269(5232):1854–1857. [PubMed: 7569924]

3. Singh S, Venkatesh S, Wang Z, et al. Diagnostic performance of magnetic resonance elastography in staging liver fibrosis: a systematic review and meta-analysis of individual participant data. Clin Gastroenterol Hepatol. 2015; 13(3):440–451. [PubMed: 25305349]

4. Dzyubak B, Glaser K, Yin M, et al. Automated liver stiffness measurements with magnetic resonance elastography. Journal of Magnetic Resonance Imaging. 2013; 38:371–379. [PubMed: 23281171]

5. Dzyubak B, Venkatesh S, Manduca A, et al. Automated liver elasticity calculation for MR elastography. J Magn Reson Imag. 2015; 43(5):1055–63.

6. Loomba R, Cui J, Wolfson T, et al. Novel 3D Magnetic Resonance Elastography for the Noninvasive Diagnosis of Advanced Fibrosis in NAFLD: A Prospective Study. Am J Gastroenterol. 2016; 111(7)

7. Andrews S, Hamarneh G, Saad A. Fast Random Walker with Priors using Precomputation for Interactive Medical Image Segmentation. Med Image Comput Comput Assist Interv. 2010; 13(3):9–16.

8. Salvado O, Hillenbrand C, Zhang S, et al. Method to Correct Intensity Inhomogeneity in MR Images for Atherosclerosis Characterization. IEEE Trans Med Imag. 2006; 25(5):539–51.

9. McGarry M, Van Houten E, Perrinez P, et al. An octahedral shear strain-based measure of SNR for 3D MR elastography. Phys Med Biol. 2011; 56:N153–64. [PubMed: 21654044]
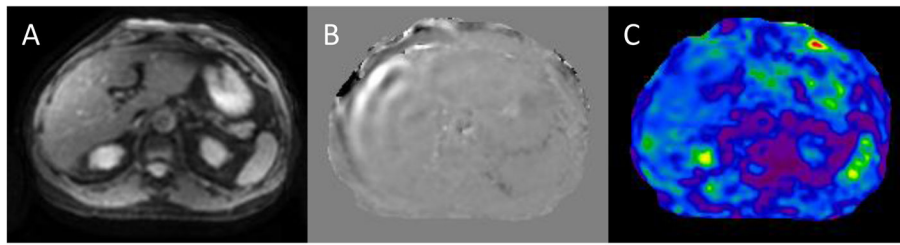
Figure 1.
Example of MRE data. A) Magnitude image showing anatomical information of the liver. B) Phase image showing wave propagation information. C) Calculated elasticity image with quantitative stiffness estimates for each voxel.
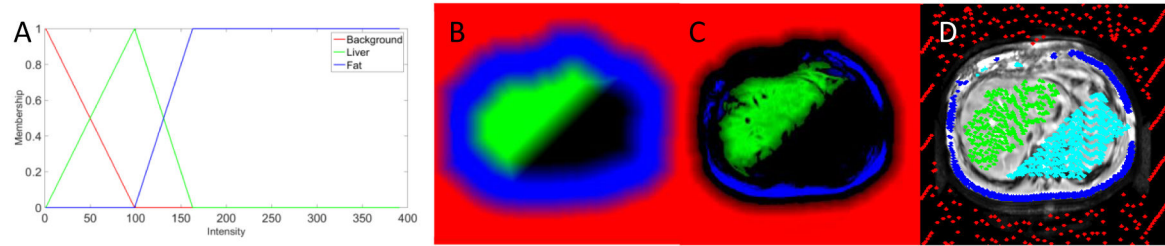
Figure 2.
Illustration of the initialization procedure. A) Intensity membership functions, B) distance membership functions, C) combined membership functions, and D) seeds subsampled from the refined initialization masks. The seeds are used as inputs for the Random Walker Segmentation.
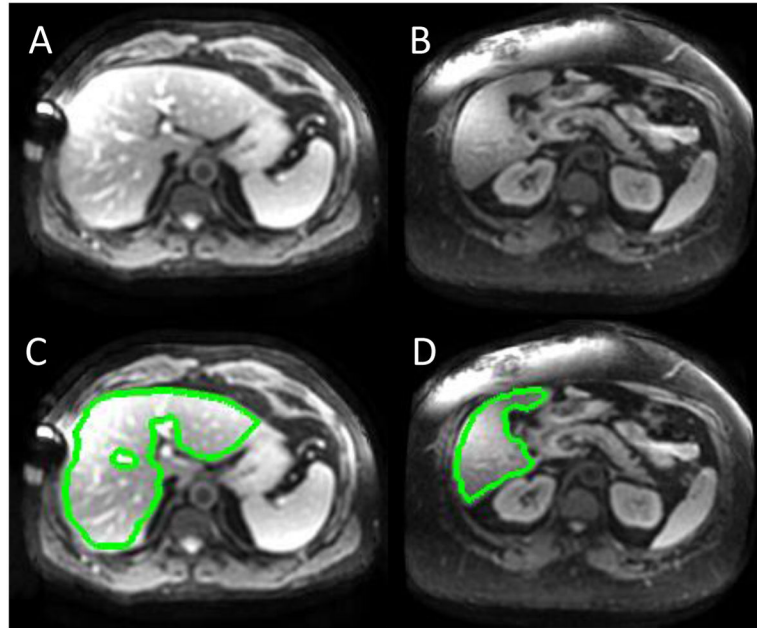
Figure 3.
Examples of 3D MRE magnitude images with moderate-low tissue contrast and intensity inhomogeneity (A and B) and the corresponding liver segmentations (C and D).
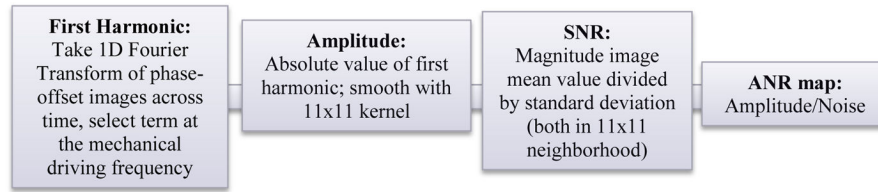
Figure 4.
Procedure for calculating the new ANR metric.
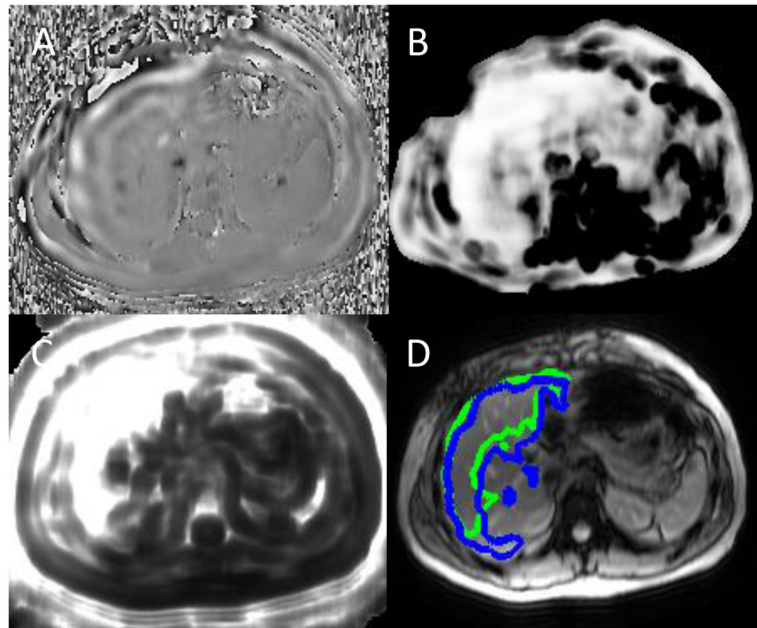
Figure 5.
Illustration of the new ANR metric with respect to the conventional confidence map. A) phase image with wave amplitude decreasing towards the medial edge of the liver, B) confidence map, C) ANR map, D) ANR mask in green corresponds well to the confidence mask in blue.
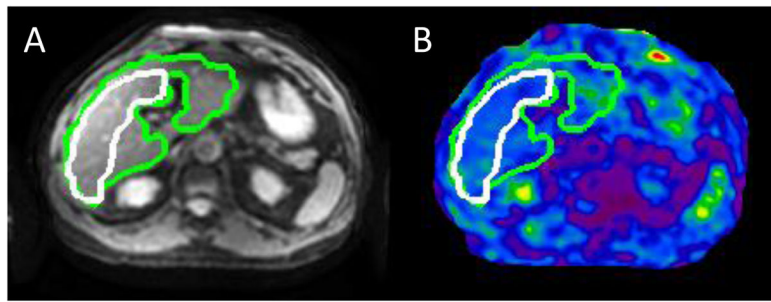
Figure 6.
An example of a manual and automated ROI for a 3D MRE exam. The magnitude (A) and elasticity (B) images are shown. The final ROIs for the reader (white) and the algorithm (green) contain only valid areas and yield stiffnesses within 2% of each other.
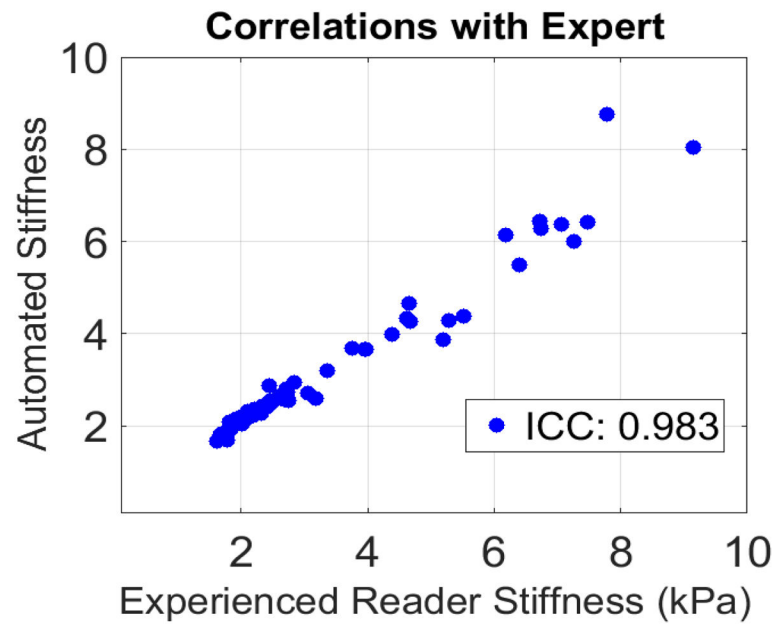
Figure 7.
Correlation of stiffnesses calculated by the expert and the automated algorithm in 57 3D MRE exams.